

Electron Overflow to the AlGaN p-Cladding Layer in InGaN/GaN/AlGaN MQW Laser Diodes

Kay Domen¹, Reiko Soejima¹, Akito Kuramata¹ and Toshiyuki Tanahashi¹
¹Fujitsu Laboratories Ltd.,

(Received Wednesday, December 24, 1997; accepted Thursday, January 29, 1998)

Current flow through an InGaN/GaN/AlGaN multi-quantum well (MQW) laser diode is simulated. We found that electron overflow to the AlGaN p-cladding layer is very large, which prevents the current injection into the MQW layers. We clarified that the electron overflow occurs easily in nitride lasers because of three intrinsic reasons; poor hole injection due to the small hole mobility and thermal velocity, the small conduction band offset for InGaN/GaN, and the high threshold carrier density. We show that the Al composition and the p-doping of the AlGaN p-cladding layer is of critical importance to obtain laser oscillation by current injection.

1 Introduction

Nakamura et al. reported 10,000 hours continuous-wave operation of nitride lasers [1] indicating that the laser is the most promising for the short-wavelength light source of the large capacity optical storages. However, it took 6 years to achieve laser diodes [2] after lasing by optical pumping at room temperature was first reported in 1990 [3]. This implies that some key issues underlying current injection have not yet been sufficiently clarified. Considering that it also took 3 years from the first commercialization of the nitride LED [4], the population inversion of carriers seems difficult for the nitride lasers. It is well known that the p-type doping has played an important role in the history of the nitride research [5] and the following realization of light emitting diodes (LED) [4]. High resistivity in p-cladding layers is still a matter of concern to nitride researchers. The hole injection then seems to be a problem.

Another unclarified issue is the band-offset for the heterojunctions. The value for the band offset is very controversial. The valence band offset for InN/GaN has been reported to be theoretically 0.51 eV by Albanesi et al. [6], 0.48 eV by Wei et al. [7], and experimentally 1.05 eV by Martin et al. [8]. We believe that the conduction band offset for InGaN/GaN is small, based on the following observations [9]: we compared two LEDs with $\text{In}_{0.13}\text{Ga}_{0.87}\text{N}/\text{GaN}$ and $\text{In}_{0.07}\text{Ga}_{0.93}\text{N}/\text{Al}_{0.05}\text{Ga}_{0.95}\text{N}$ double-hetero structures, both of which have the same bandgap difference between the active and the cladding layer. On current injection, the InGaN/

GaN LED showed a weak active layer luminescence and relatively strong deep-level luminescence in the GaN p-cladding layer. These results indicated that the electron overflow to the p-cladding layer disturbs the current injection to the active layer. In contrast, the InGaN/AlGaN showed strong active-layer luminescence. Since photoluminescence intensities were comparable for the two structures, we believe the conduction band offset is smaller for InGaN/GaN than for InGaN/AlGaN. The value for the ratio of conduction band offset to valence band for InN/GaN of 3:7 reported by Martin et al. [8] explains these results well. This implies that electron overflow occurs easily in nitride lasers. Therefore, the hole injection and electron overflow may be what makes the population inversion of carriers difficult. However, current flow in the laser has not been sufficiently studied.

In this paper, we analyzed the bands and the carrier distribution self-consistently in an InGaN/GaN/AlGaN MQW laser diode, and simulated current flow through the laser structure to investigate current paths that disturb the laser oscillation. We found that serious electron overflow to the p-cladding layer takes place in the nitride lasers.

2 Simulation of Overflow Leak Current

We used a ready-made device simulator, LASTIP [10], and we assumed:

- MQWs consisting of:
- five pairs of 2-nm thick $\text{In}_{0.15}\text{Ga}_{0.85}\text{N}$ wells and 5-nm thick $\text{In}_{0.03}\text{Ga}_{0.97}\text{N}$ barriers

- 0.1- μm thick GaN SCH layers
- $\text{Al}_x\text{Ga}_{1-x}\text{N}$ cladding layers
- a $\Delta E_c:\Delta E_v$ ratio for InGaN/GaN of 3:7
- an electron mobility of $200\text{ cm}^2/\text{Vs}$ for all layers
- hole mobility of $8\text{ cm}^2/\text{Vs}$ for the p-SCH layer
- hole mobility of $6\text{ cm}^2/\text{Vs}$ for the p-cladding layer
- nonradiative lifetime in the well layer of 1 ns
- nonradiative lifetime in the the p-cladding layer of 0.1 ns

Since reported $\Delta E_c:\Delta E_v$ ratios for GaN/AlGaIn are scattered [6] [7] [8] [11] [12] [13] [14] [15], we assumed the value 5:5. Since we believe that the lasing takes place by free carriers [16], we assumed a radiative coefficient, B , of $2 \times 10^{-10}\text{ cm}^3/\text{s}$ for all layers, based on the theoretical calculation for GaN [17]. We varied the Al composition and p-doping concentrations in the p-cladding layer and the device temperature.

We first simulated a structure having an $\text{Al}_{0.05}\text{Ga}_{0.95}\text{N}$ p-cladding layer with a p-doping concentration of $2 \times 10^{17}\text{ cm}^{-3}$ at 300 K. The bandgap difference between the well and the cladding layer (ΔE_g) was 500 meV. Figure 1 shows the leakage current due to the electron overflow to the p-cladding layer and the active layer current as functions of the total current. Since the active layer current includes the radiative and nonradiative current in both the MQW and the SCH layers, the threshold active layer current for the laser oscillation was $12\text{ kA}/\text{cm}^2$ assuming a threshold loss of 50 cm^{-1} . This value of threshold current is reasonable, because an MQW with wells thinner and more numerous requires a higher threshold current [17]. We should note that this threshold current density corresponds to the local current density where optical gain is generated. This is larger than experimentally observed macroscopic threshold current densities, because current density is not homogeneous in the well layers due to the composition fluctuation of InGaIn [18] [19]. From Figure 1, we found that the overflow current increases rapidly as total current increases. At a total current of $20\text{ kA}/\text{cm}^2$, the overflow current becomes more than half of that. This large overflow prevents the increase of the active layer current, causing a high threshold total current density (J_{th}) of $37\text{ kA}/\text{cm}^2$. The result indicates that the electron overflow takes place easily for the nitride laser, because a ΔE_g of 500 meV is generally considered to be sufficient for conventional III-V lasers. An LED does not suffer from the leakage current, since it is operated at a current density under $1\text{ kA}/\text{cm}^2$. We think this is one of the reasons why bright LEDs do not always produce lasing.

We then simulated the leakage while varying the Al composition in the p-cladding layers, x , as 0.05, 0.1, 0.15, and 0.2 with corresponding ΔE_g of 500, 640, 780, and 920 meV, respectively. Figure 2 shows the overflow leakage current as a function of the total current at various Al compositions. Device temperature and p-doping concentration were again fixed at 300 K and $2 \times 10^{17}\text{ cm}^{-3}$. We found that the leakage current is significantly reduced by the increase of Al composition. The current density where leakage starts increases as Al composition increases. We also found that we need ΔE_g of about 800 meV to sufficiently suppress the leakage current.

Next, we examined the effect of the p-doping concentration (N_p) in the cladding layer. The Al composition was fixed at 0.1. Figure 3 shows the leakage current for a N_p of $2 \times 10^{17}\text{ cm}^{-3}$ and $1 \times 10^{18}\text{ cm}^{-3}$. We found that leakage rapidly increases as N_p decreases. Although we could not calculate leakage under $1 \times 10^{17}\text{ cm}^{-3}$ in the high current injection regime due to the convergence difficulty, the leakage calculated for $5 \times 10^{16}\text{ cm}^{-3}$ under low current injection showed a very large increase. Since p-doping concentration generally decreases as Al composition increases, these two are trade-off parameters. Thus, an optimum Al composition will exist to minimize the leakage current.

Finally, we simulated the influence of the temperature of the laser diode. Figure 4 shows the overflow leakage current when we set a constant temperature of 300, 350, and 400 K on a device. We found that the influence of the temperature becomes pronounced in higher injection range. In reality, this large leakage under high current injection generates heat, which results in further leakage. Once this positive feedback occurs, the leakage becomes the dominant current path, and carrier density in the active layer does not increase with the current, and laser oscillation never appears. In contrast, the influence of the temperature is small in the lower current range. This means that when we sufficiently reduce the threshold current density, the leakage will not occur even at higher temperature.

3 Why Electrons Overflow

In this section we analyze how electrons leak by checking a band diagram of the laser diode. Figure 5 shows a band diagram under laser oscillation with an Al composition and p-doping concentration in the cladding layer of 0.1 and $2 \times 10^{17}\text{ cm}^{-3}$ at 300 K. The output power is 15 mW and the operation voltage is 9 V for the diagram. The right-hand side is the p-side. The dashed lines are quasi-Fermi levels. The inset is the magnified view of the valence band around the MQW. We found a large discontinuity in the hole Fermi level between the p-SCH

layer and the MQW, indicating poor hole injection into the MQW from the SCH layer. This poor hole injection occurs because hole mobility and thermal velocity are small due to the large hole masses of nitride materials. Then the current flow over the heterojunction between the p-SCH and the MQW becomes small resulting in the large Fermi level discontinuity. The poor hole injection into the MQW also causes the large hole density at the p-SCH layer, which attracts electrons to the p-side. In this way, Fermi levels are higher in the p-side SCH layer than in the n-side both for the conduction and valence bands. We also found that the slope of the p-cladding layer is large due to the high resistivity.

Next we looked at the distribution of the hole and electron densities across the laser structure. Figure 6 shows the hole density distribution at the same situation as that in the band diagram. The transverse axis is the same as that in Figure 5. We found that the hole density at the p-SCH layer reaches over 10^{18} cm^{-3} . We also found that the hole densities in the well layers are inhomogeneous reflecting the poor hole injection. Figure 7 shows the electron density distribution. The electron density is larger in the p-side SCH layer than in the n-side SCH. This large electron density at the p-side SCH layer is caused by the following three factors: first, the poor hole injection described above, second, the small band-offset ratio (0.3) of the conduction band between InGaN and GaN, and third, the high threshold carrier density of over $1 \times 10^{19} \text{ cm}^{-3}$. Regarding the third factor, the electron Fermi level must be raised higher to make population inversion, since the hole Fermi level is not easily raised. This is because there are three bands in the valence band, two of which have very large effective masses. In this way, the electron density becomes large in the p-SCH layer. It becomes more than 10^{18} cm^{-3} near the interface of the p-SCH and p-cladding layer and serious overflow of over 10^{15} cm^{-3} to the p-cladding layer takes place. The overflow is enhanced by the high electric field caused by the high resistivity in the p-cladding layer. From Figure 7, we also found that electron injection is inhomogeneous in the well layers. It increases towards the p-side, as in the hole case. These inhomogeneous injections of carriers will cause inhomogeneous generation of the optical gain.

From the results described above, there are three intrinsic causes for the large electron overflow in the nitride lasers: the poor hole injection due to the small thermal velocity and mobility of the holes, the small conduction band offset for InGaN/GaN, and the large threshold carrier density. These are intrinsic to nitride materials; we can not avoid them. Therefore, it is very important to improve the three non-intrinsic factors: low

Al composition, high resistivity, and short carrier lifetime in the p-cladding layer.

4 Conclusion

In summary, we found that electrons easily overflow to the p-side layers in nitride lasers because of three intrinsic reasons:

1. poor hole injection
2. the small conduction band offset of InGaN/GaN, and
3. the high threshold carrier density.

We showed that this leakage disturbs the current injection to the MQW, and that a high Al composition and p-doping in the p-cladding layer is of critical importance to injection.

REFERENCES

- [1] S. Nakamura, M. Senoh, S. Nagahama, N. Iwasa, T. Yamada, and T. Matsushita, Post deadline Papers of IEEE Lasers and Electro-Optics Society, PD1.1 (1997)
- [2] S. Nakamura, M. Senoh, S. Nagahama, N. Iwasa, T. Yamada, T. Matsushita, H. Kiyoku, Y. Sugimoto, *Jpn. J. Appl. Phys.* **35**, L74-L76 (1996).
- [3] H. Amano, T. Asahi, I. Akasaki, *Jpn. J. Appl. Phys.* **29**, L205 (1990).
- [4] Shuji Nakamura, Masayuki Senoh, Takashi Mukai, *Appl. Phys. Lett.* **62**, 2390-2392 (1993).
- [5] S. Strite, H. Morkoç, *J. Vac. Sci. Technol. B* **10**, 1237-1266 (1992).
- [6] E. A. Albanesi, W. R. L. Lambrecht, B. Segall, *J. Vac. Sci. Technol. B* **12**, 2470-2474 (1994).
- [7] SH Wei, A. Zunger, *Appl. Phys. Lett.* **69**, 2719-2721 (1996).
- [8] G. Martin, A. Botchkarev, A. Rockett, H. Morkoc, *Appl. Phys. Lett.* **68**, 2541-2543 (1996).
- [9] R. Soejima, unpublished.
- [10] LASTIP Manual Ver. 3.4 (Crosslight Software Inc., 1995)
- [11] J. Baur, K. Maier, M. Kunzer, U. Kaufmann, J. Schneider, *Appl. Phys. Lett.* **65**, 2211-2213 (1994).
- [12] G. Martin, S. Strite, A. Botchkarev, A. Agarwal, A. Rockett, H. Morkoc, W. R. L. Lambrecht, B. Segall, *Appl. Phys. Lett.* **65**, 610-612 (1994).
- [13] J. R. Waldrop, R. W. Grant, *Appl. Phys. Lett.* **68**, 2879-2881 (1996).
- [14] A. Salvador, G. Liu, W. Kim, O. Aktas, A. Botchkarev, H. Morkoc, *Appl. Phys. Lett.* **67**, 3322-3324 (1995).
- [15] A. Bykhovski, B. Gelmont, M. Shur, A. Khan, *J. Appl. Phys.* **77**, 1616-1620 (1995).
- [16] K. Domen, A. Kuramata, and T. Tanahashi, Proceedings of the Second International Conference on Nitride Semiconductors, 236 (Tokushima, 1997)
- [17] K. Domen, K. Horino, A. Kuramata, and T. Tanahashi, Digest of the LEOS Summer Topical Meetings, Gallium Nitride Materials, Processing, and Devices, 35 (1997)
- [18] S. Chichibu, T. Azuhata, T. Sota, S. Nakamura, *Appl. Phys. Lett.* **69**, 4188-4190 (1996).
- [19] Y. Narukawa, Y. Kawakami, M. Funato, S. Fujita, S. Fujita, S. Nakamura, *Appl. Phys. Lett.* **70**, 981-983 (1997).

FIGURES

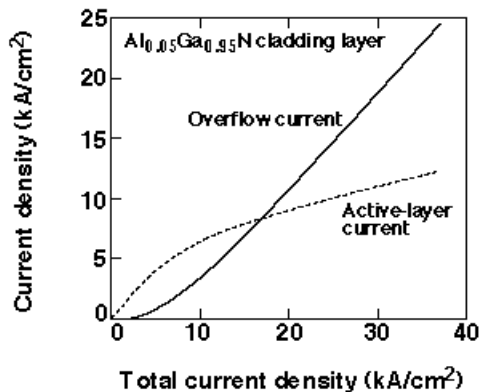


Figure 1. Leakage current due to the overflow to the p-cladding layer and current injected into the MQW layer as functions of total current. Leakage starts in the low current region. Although the threshold active layer current for the laser oscillation is 12 kA/cm², large overflow causes a high threshold total current density of 37 kA/cm².

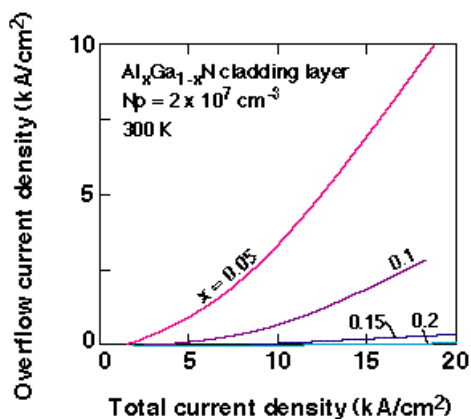


Figure 2. Overflow current as a function of total current at various Al compositions. The current density where leakage starts increases as Al composition increases. We need ΔE_g of about 800 meV to sufficiently suppress the leakage current.

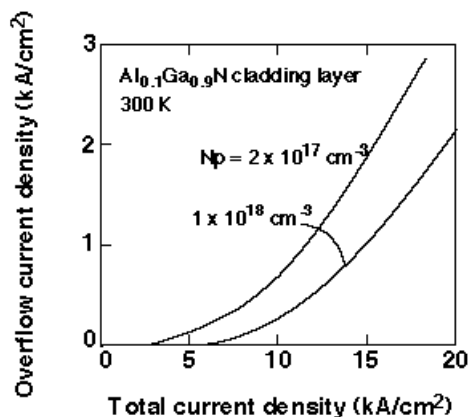


Figure 3. Overflow current as a function of total current at various p-concentrations.

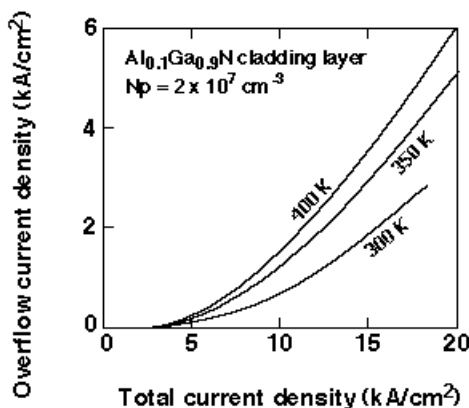


Figure 4. Overflow current as a function of total current at various temperatures. The influence of the temperature becomes pronounced in higher injection range.

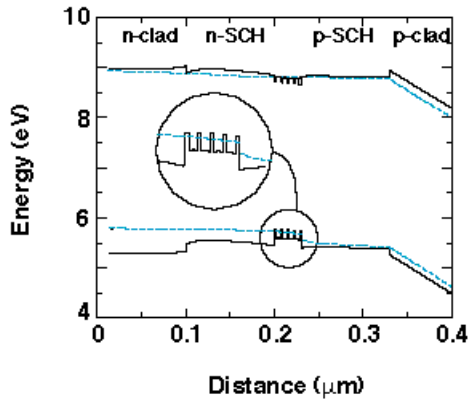


Figure 5. Band diagram under laser oscillation. The dashed lines are quasi-Fermi levels and the inset is the magnified view of the valence band around the MQW. A large discontinuity in the hole Fermi level between the p-SCH layer and the MQW and large electric field in the p-cladding layer are observed.

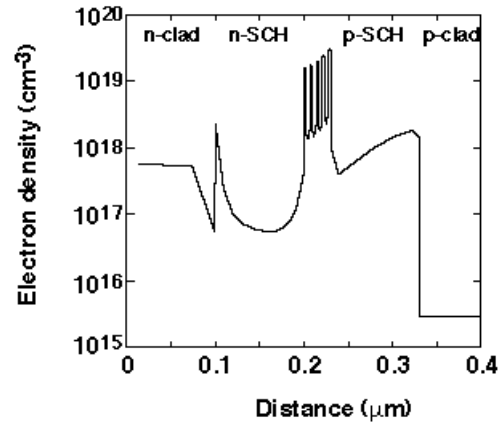


Figure 7. Electron density distribution. The electron density is larger in the p-side SCH layer than in the n-side SCH.

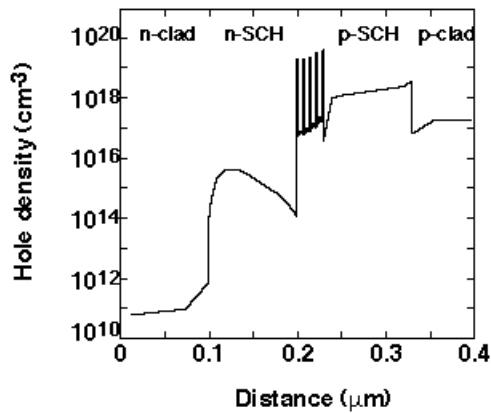


Figure 6. Hole density distribution at the same situation as that in the band diagram. Hole density at the p-SCH layer reaches over 10^{18} cm^{-3} and that in the well layers are inhomogeneous in each well.